Molecular Crystals and Liquid Crystals Science and Technology. Section A. Molecular Crystals and Liquid Crystals
Publication details, including instructions for authors and subscription information:
http://www.tandfonline.com/loi/gmcl19

# Thermodynamical Properties of Bicomponent Mixtures of Liquid Crystals Cholesteryl Pelargonate and Nonyloxybenzoic Acid

S. L. Srivastava [a] , Ravindra Dhar [a] & Arunima Mukherjee [a]
[a] Physics Department, University of Allahabad, Allahabad, 211002, India

Version of record first published: 24 Sep 2006.

To cite this article: S. L. Srivastava , Ravindra Dhar & Arunima Mukherjee (1996): Thermodynamical Properties of Bicomponent Mixtures of Liquid Crystals Cholesteryl Pelargonate and Nonyloxybenzoic Acid, Molecular Crystals and Liquid Crystals Science and Technology. Section A. Molecular Crystals and Liquid Crystals, 287:1, 139-154

To link to this article: http://dx.doi.org/10.1080/10587259608038751

*Mol. Cryst. Liq. Cryst.*, 1996, Vol. 287, pp. 139–154
Reprints available directly from the publisher
Photocopying permitted by license only





# Thermodynamical Properties of Bicomponent Mixtures of Liquid Crystals Cholesteryl Pelargonate and Nonyloxybenzoic Acid

S. L. SRIVASTAVA, RAVINDRA DHAR and ARUNIMA MUKHERJEE

*Physics Department, University of Allahabad, Allahabad-211002, India*

*(Received March 11, 1994; in final form February 7, 1996)*

Transition temperatures, transition enthalpies and entropies of different mesophases of the binary mixture of cholesteryl pelargonate (ChP) and nonyloxybenzoic acid (NOBA) have been measured on a differential scanning calorimeter and optical textures of different mesophases have been confirmed on a polarizing microscope. Eutectic point has been observed at $28 \pm 2$ mole percent of NOBA from the variation of transition temperature, enthalpy and entropy of the crystal to mixed crystal phase and the mixed crystal phase to mesophase with concentration of NOBA. Stability of SmA phase increases on addition of NOBA. SmA* phase has been observed in between SmA and Ch phases for NOBA concentrations between 18 and 50 mole percent. A very wide cholesteric range of about 50 °C has been observed in cooling in the concentration range of 60 to 90 mole percent of NOBA.

*Keywords: Liquid crystal mixture, thermodynamics, eutectic, cholesteryl pelargonate, nonyloxybenzoic acid.*

## INTRODUCTION

Binary liquid crystal mixtures exhibit induced and reentrant mesophases[1,2] which does not conform to the simple eutectic phase diagram. Binary mixtures in which one component is a cholesteryl ester have been of considerable interest in the recent past[1,3–7]. In the binary mixtures of cholesteryl esters, Palangana *et al.*[8] have observed a second order smectic-A (SmA) to cholesteric (Ch) phase transition and a tricritical point in the 50:50 mole percent of cholesteryl pelargonate and cholesteryl caproate. There is also a possibility of induced ferroelectric helical smectic-C (SmC*) phase in the mixtures of two optically active cholesterol derivatives[7]. In the nematic-cholesteric mixtures, consisting of a cholesteryl ester and nonyloxybenzoic acid, Lisetsky *et al.*[1] have observed a very fast depression of SmC transition temperature. Lavrentovich and Nastishin[3] have measured the coefficient of viscosity and surface tension of the dispersed drops of cholesteryl pelargonate (ChP) and nonyloxybenzoic acid (NOBA) mixture (70:30 weight fraction) in lecithin-glycerin and observed for the first time a superconducting type-II phase in between the cholesteric and

SmA phases of the mixture which agrees with 3-dimensional quasicrystalline phase called as Z-and ZZ-phases by these authors and later they observed SmA* phase[4]. In this communication we report a comprehensive thermodynamical study for the various concentrations of this mixture.

## EXPERIMENTAL DETAILS

Pure grade samples of cholesteryl pelargonate and nonyloxybenzoic acid were procured from Institute of Physics, Academy of Sciences of Ukraina, Kiev and they were used as such without any further purification. Thermodynamical study of the binary mixtures of different concentrations were made on a Perkin-Elmer Differential Scanning Calorimeter (model DSC-7) which has a built-in soft-ware 'PEAK' to determine the peak transition temperature, the onset temperature and the transition enthalpy. The mixtures were prepared from weighed out portions of the pure components and were homogenized before taking the measurements by heating to a temperature several degrees above the transition to the isotropic phase, stirring and finally cooling. To purge any impurity around the sample in the sample holder, nitrogen gas was flown in at about 25–30 lb/inch$^2$ (PSI) pressure. The DSC was allowed to run at the scanning rate of 5 °C/min for the first five cycles in the temperature range of 30–150 °C to stabilize the transition temperatures and the transition heats. When these values were found to be stabilized, the DSC was run at different scanning rates between 2.5 °C/min and 15 °C/min.

Highly pure indium and zinc have been used as standard calibrants after making the initial runs for the slope and baseline adjustments. Maximum accuracy in the transition temperature is $\pm 0.1$ °C and in transition enthalpy it is about 5% in the organic compounds. The phase transitions are verified in both heating and cooling cylces by their characteristic optical textures with the help of a polarizing microscope (CENSICO model) fitted with a hot-stage. Different mesophases including the blue phase have been observed.

## RESULTS AND DISCUSSION

Linear graphs between transition temperature and scanning rate have been plotted using the least square fit method because the transition temperatures of different mesophases depend linearly on the scanning rates[9,10]. Intercept of the straight line on the temperature axis gives the true transition temperature at the extrapolated scanning rate of 0 °C/min. The phase diagrams thus obtained are shown in Figure 1(a) and (b). The phase diagrams ($T_P$ vs $x$) of the two-component system NOBA-ChP determined by DSC in both heating and cooling runs respectively are in agreement with those determined by the polarizing microscopy which reveal more details about the mixed phases.

Pure ChP exhibits a monotropic SmA phase. In heating, it shows phase transitions: K (78.2) Ch (89.7) I and in cooling I (89.8) Ch (74.0) SmA (overnight cooling)

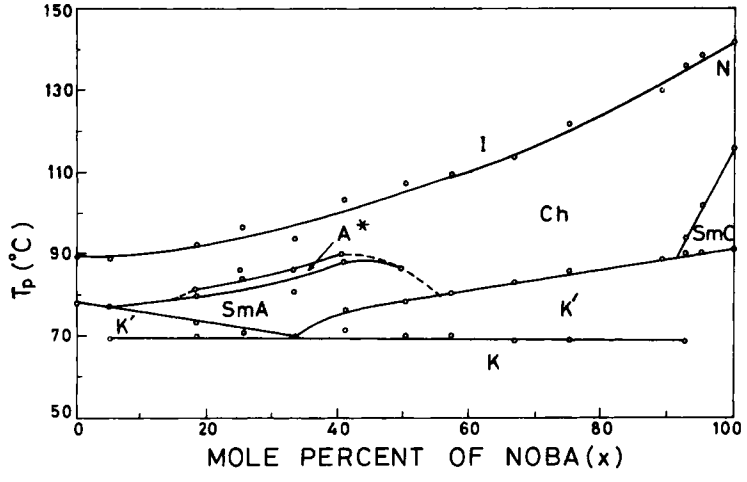


(a)

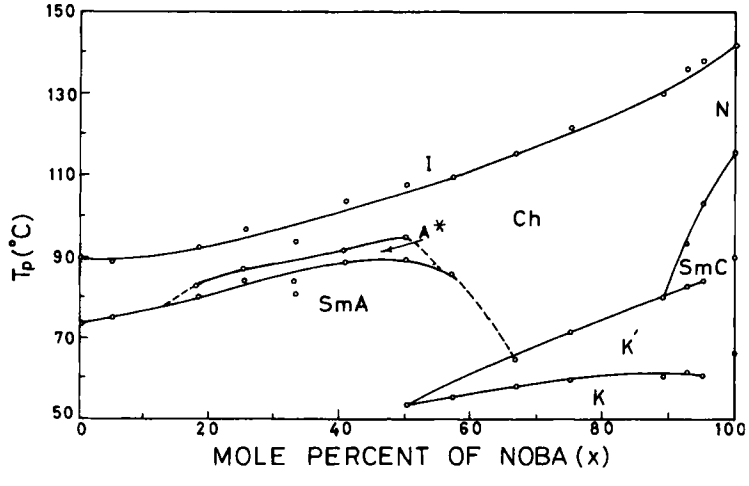


(b)

FIGURE 1 Phase diagram of the mixture ChP + NOBA, transition temperature as a function of concentration of NOBA ($x$),(a) heating, (b) cooling. The dashed portions of the curves represent extrapolations.

K, whereas pure NOBA which is enantiotropic, shows the phase transitions: K (91.2) SmC (115.8) N (141.8) I. Transition temperatures in °C are given in parenthesis.

The melting thermogram of the mixture in the solid phase exhibits two unresolved peaks which merge with each other in the eutectic region. The thermogram is manually resolved into two curves. The area under each curve (which is directly related to the transition enthalpy) is determined. The transition enthalpies of the doublet so determined are listed in Table 1.

The first peak appearing at 70 °C is almost invariant with concentration of NOBA and represents the melting of crystal phase (K) to a mixed crystal-mesophase (K').

TABLE 1

Transition temperatures, transition enthalpies, transition entropies and half-widths of transitions for different mole percents of NOBA in heating. * — by weight method, rest by 'PEAK' method.

| *Mole %* | $T_P$(°C) | $\Delta H$(*kJ/mole*) | $\Delta S$(*J/mole − K*) | $\Delta T$(°C) |
|---|---|---|---|---|
| | | $K - K'$ | | |
| 0 | — | — | — | — |
| 4.67 | 69.4 | 3.25* | 9.49 | 1.7 |
| 18.18 | 69.8 | 17.2* | 50.2 | 1.4 |
| 25.35 | 70.6 | 24.4 | 70.9 | 2.1 |
| 33.33 | 69.9 | 22.6 | 65.8 | 1.8 |
| 40.68 | 71.1 | 23.8* | 69.2 | 2.2 |
| 50.17 | 70.0 | 20.9* | 60.8 | 1.9 |
| 56.98 | 69.7 | 16.1* | 47.1 | 2.3 |
| 66.55 | 68.5 | 12.7* | 37.2 | 2.6 |
| 74.92 | 68.9 | 9.48* | 27.7 | 2.2 |
| 88.86 | 63.3 | 1.83 | 5.43 | 3.8 |
| 92.55 | 68.7 | 2.05 | 5.98 | 2.0 |
| 95.10 | 68.6 | 0.72 | 2.10 | 1.8 |
| 100 | — | — | — | — |
| | | $K'$-Mesophase | | |
| 0 | 78.2 | 23.3 | 66.2 | 1.1 |
| 4.67 | 77.3 | 17.0* | 48.6 | 2.2 |
| 18.18 | 73.2 | 5.4* | 15.5 | 2.6 |
| 25.35 | — | — | — | — |
| 33.33 | — | — | — | — |
| 40.68 | 76.3 | 3.5* | 10.0 | 2.8 |
| 50.17 | 78.4 | 6.9* | 19.6 | 5.8 |
| 56.98 | 80.4 | 10.5* | 29.8 | 8.6 |
| 66.55 | 83.2 | 17.5* | 49.2 | 6..6 |
| 74.92 | 85.7 | 22.5* | 62.6 | 6.1 |
| 88.86 | 88.5 | 27.2 | 75.2 | 4.1 |
| 92.55 | 90.0 | 26.4 | 72.7 | 1.6 |
| 95.10 | 90.3 | 28.5 | 78.5 | 1.7 |
| 100 | 91.2 | 32.7 | 89.7 | 1.3 |
| | | Sm-Ch | | |
| 0 | — | — | — | — |
| 4.67 | — | — | — | — |
| 18.18 | 79.9 | 0.404 | 1.14 | — |
| 25.35 | 84.0 | 0.419 | 1.17 | — |
| 33.33 | 80.7 | 0.399 | 1.13 | — |
| 40.68 | 88.2 | 0.306 | 0.847 | — |
| 50.17 | 86.5 | 0.226 | 0.630 | — |
| 56.98 | — | — | — | — |
| 66.55 | — | — | — | — |
| 74.92 | — | — | — | — |
| 88.86 | — | — | — | — |
| 92.55 | 94.1 | 0.434 | 1.18 | — |
| 95.10 | 102.1 | 0.695 | 1.84 | — |
| 100 | 115.8 | 1.56 | 4.01 | — |
| | | Ch-I | | |
| 0 | 89.7 | 0.647 | 1.78 | 0.5 |
| 4.67 | 88.9 | 0.821 | 2.27 | 0.5 |
| 18.18 | 92.3 | 0.885 | 2.42 | 0.5 |
| 25.35 | 96.6 | 1.02 | 2.75 | 0.8 |
| 33.33 | 93.8 | 0.967 | 2.63 | 0.9 |

TABLE 1 *(Contd.)*

| | | | | |
|---|---|---|---|---|
| 40.68 | 103.3 | 1.09 | 2.91 | 1.7 |
| 50.17 | 107.2 | 1.09 | 2.86 | 2.2 |
| 56.98 | 109.3 | 1.27 | 3.31 | 2.2 |
| 66.55 | 113.8 | 1.39 | 3.61 | 2.6 |
| 74.92 | 121.6 | 1.70 | 4.32 | 2.2 |
| 88.86 | 129.8 | 2.07 | 5.13 | 3.4 |
| 92.55 | 136.0 | 2.35 | 5.73 | 1.1 |
| 95.10 | 138.3 | 1.99 | 4.83 | 0.9 |
| 100 | 141.8 | 2.26 | 5.46 | 0.6 |

The enthalpy and entropy of this transition show a maximum at 28 mole percent of NOBA (see Fig. 2 and 3). The second peak corresponds to transition from the mixed phase to a mesophase and its transition temperature shows a minimum at 30 mole percent of NOBA (see Fig. 1(a)). For this K′-mesphase transition, both enthalpy and entropy show a minimum at 27 mole percent of NOBA (see Fig. 2 and 3). Hence the eutectic composition may be taken as $28 \pm 2$ mole percent of NOBA. Eutectic composition has been calculated with the help of an empirical equation[11]

$$x_e = \frac{100(T_2 - T_e)}{T_1 + T_2 - 2T_e} \tag{1}$$

where $T_1$ and $T_2$ are melting points of the lower and higher melting components of the binary mixture, $T_e$ is the eutectic temperature and $x_e$ is the eutectic mole percent of the lower melting component (ChP), which gives $x = 71$ mole percent ChP. The

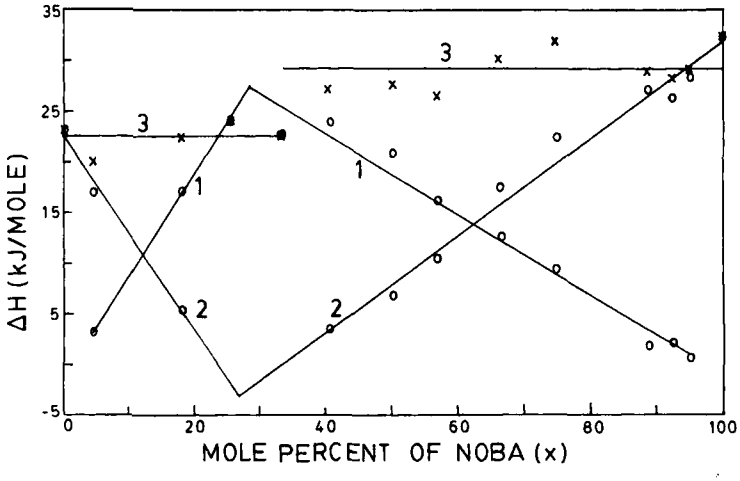


FIGURE 2 Transition enthalpy as a function of mole percent of NOBA ($x$) in heating. Curve 1 represents K-K′ transition, curve 2 K′-Mesophase transition and curve 3 sum of enthalpies of K-K′ and K′-Mesophase transitions.

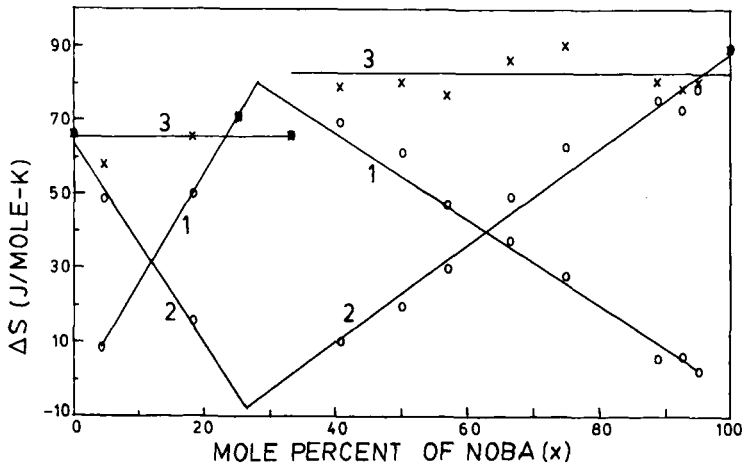


FIGURE 3 Transition entropy as a function of mole percent of NOBA (x) in heating. Curve 1 represents K-K′ transition, curve 2 K′-Mesophase transition and curve 3 sum of entropies of K-K′ and K′-Mesophase transitions.

calculated eutectic composition from equation (1) is ChP:NOBA as 71:29 which agrees with the experimental value. Eutectic composition has also been calculated by Schroder-Van Laar equation[11,12]

$$\ln x = \frac{\Delta H}{R}\left(\frac{1}{T_1} - \frac{1}{T_e}\right) - \ln f_i \tag{2}$$

where $\Delta H$ is the crystal to mesophase transition enthalpy of ChP, $R$ is the gas constant and $f_i$ is the activity coefficient and is 1 for ideal mixed phases[12]. Taking $f_i = 1$, $x_e$ comes out to be 82 mole percent of ChP. We may however note that molecular length of ChP is almost twice that of NOBA, hence it may not be ideal case and therefore taking $f_i = 1.06$ ($R \ln f_i = 0.5$)[12], $x_e$ comes out to be 22 mole percent of ChP. For $x_e = 72$ mole percent of ChP (eutectic composition) $f_i$ should be 1.15. Hence it seems that Schroder-Van Laar equation which involves many approximations[12] is applicable to this system only if non ideal mixing term is taken into account. Solid state polymorphism of NOBA in crystal phase may also cause discrepancy in the calculated results[13].

In cooling, pure NOBA goes into two cyrstalline phases (see Fig. 1(b)) while pure ChP goes into one crystalline phase usually after overnight cooling at room temperature. Range of the mixed crystal phase decreases with the increasing concentration of ChP and disappears at about 44 mole percent of ChP. Both enthalpy and entropy for (K′-K) as well as for (Mesophase-K′) transitions decrease with increasing concentration of ChP (see Fig. 4 and 5).

The sum of enthalpies and the sum of entropies for K-K′ and K′-Mesophase transitions are $22.6 \pm 0.96$ kJ/mole and $65.4 \pm 2.9$ J/(mole-K) respectively before the eutectic point (agreeing with that of pure ChP) and the values are $29.3 \pm 1.6$ kJ/mole

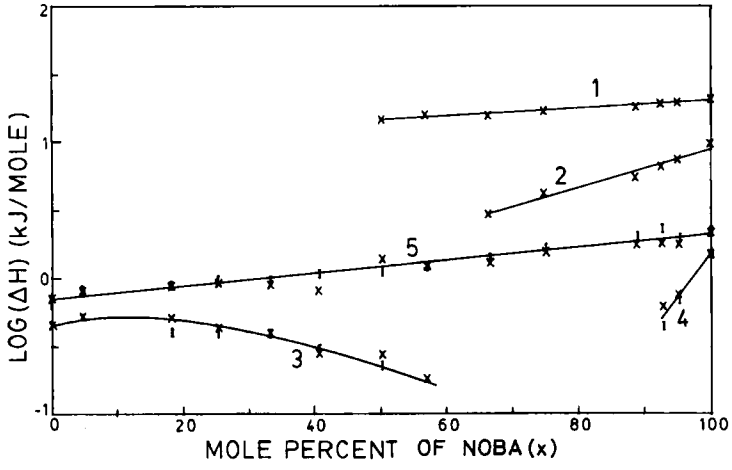


FIGURE 4 Log of transition enethalpy as a function of mole percent of NOBA ($x$). Curve 1 represents K'-K transition, curve 2 Mesophase-K' transition, curve 3 SmA-Ch (Ch-SmA) transition, curve 4 SmC-Ch (Ch-SmC) transition and curve 5 Ch-I (I-Ch) transition. Experimental data in heating are shown by (I) and in cooling by ($x$).

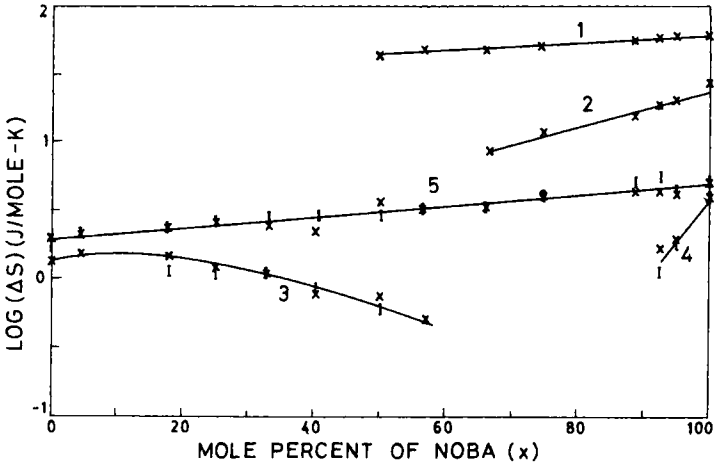


FIGURE 5 Log of transition entropy as a function of mole percent of NOBA ($x$). Curve 1 represents K'-K transition, curve 2 Mesophase-K' transition, curve 3 SmA-Ch (Ch-SmA) transition, curve 4 SmC-Ch (Ch-SmC) transition and curve 5 Ch-I (I-Ch) transition. Experimental data in heating are shown by (I) and in cooling by ($x$).

and $82.5 \pm 4.2$ J/(mole-K) respectively after the eutectic point (agreeing to that of pure NOBA) thereby showing an abrupt jump of enthalpy and entropy in the eutectic region (see Fig. 2 and 3). It may therefore be inferred that before the eutectic point the crystalline behaviour of the mixture resembles almost to that of ChP and after the eutectic point it becomes similar to that of NOBA.

## SmA and A* Phases

In heating, SmA phase appears at around 10 mole percent and it disappears above 50 mole percent of NOBA (see Fig. 1 (a)), while in cooling SmA phase, which is characteristic of pure ChP, disappears around 67 mole percent of NOBA (see Fig. 1(b)). Transition temperatures of SmA phase increase upto 41 mole percent of NOBA and there after decrease showing that stability of SmA phase increases due to addition of NOBA upto 41 mole percent, but further addition of NOBA destabilizes SmA phase. It may be noted that transition temperatures of SmA phase show appreciable depression from the smooth curve in the eutectic region (see Fig. 1(a) and (b)).

The enthalpy and entropy of SmA-Ch transition show a peak around 20 mole percent of NOBA (see Fig. 4 and 5). Decrease in the enthalpy and entropy above 20 mole percent of NOBA show that miscibility of ChP and NOBA molecules decreases and is completely broken above 56 mole percent of NOBA resulting in suppression of SmA phase and emergence of a large cholesteric gap separating SmA and SmC phases[2]. However, the DSC thermograms of Ch-SmA phase transitions are quite weak and broad, making the measurements difficult.

A careful examination of Ch-SmA transition curves show a small shoulder on the higher temperature side for NOBA compositions of 18.18, 25.35, 33.33, 40.68 and 50.17 mole percents, which are separated by about 2–4 °C (see Fig. 6). By optical, acoustical, X-ray, viscoelastic and DSC studies Lavrentovich *et al.*[4] have observed helical SmA (A*) phase between Ch and SmA phases of the mixture of composition 42 mole percent of NOBA in ChP. From their X-ray studies they find the width of SmA* phase to be about 7 °C, but from the acoustical and DSC studies it seems to be about 2 to 4 °C. In their DSC thermogram SmA-A* and A*-Ch peaks are not resolved and total latent heat of both peaks is 0.27 kJ/mol. The higher temperature side shoulder of this curve is therefore taken to be Ch-SmA* transition. In our DSC thermograms maximum width of A* phase is about 5 °C and Ch-SmA* transition enthalpy is not more than 0.055 kJ/mole. SmA* phase is shown in Figure 1(a) and (b) with an approximate width of 2–4 °C.

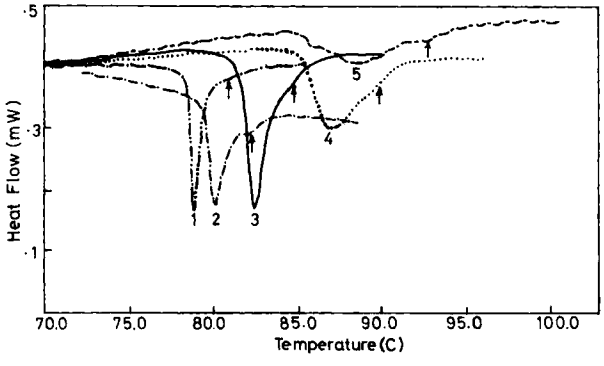


FIGURE 6 DSC thermograms for SmA transition at different mole percent of NOBA. (↑) indicates Ch-SmA* transition, Curve 1 represents the transitions at 18.18 mole percent, Curve 2 at 25.35, Curve 3 at 33.33, Curve 4 at 40.68 and Curve 5 at 50.17 mole percent.

The binary system of ChP and NOBA molecules exhibiting polymorphism does not seem to form a complex. It seems that the functional groups, the shape and size of ChP and NOBA molecules are responsible for the smectic A packing[14,15]. The molecules of ChP are stacked with each other in antiparallel arrangement in the crystal phase[16] and perhaps also in SmA phase. NOBA molecules form doubly hydrogen-bonded dimer with a small percentage of monomer or dimer with one broken hydrogen bond[17]. NOBA molecules have the length almost half of ChP molecules and hence it seems that two NOBA molecules in a head to head arrangement with the carboxyl groups adjacent to each other forming the doubly hydrogen bonds may occupy the space between ChP molecules on the basis of structural arrangement and dipolar interactions in such a way that the occupied volume and energy of configuration is minimum. A possible arrangement is shown in Figure 7. Because of such lengths of NOBA and ChP molecules, even a small concentration of NOBA may lead to a locked phase region in the real space representation[18]. The dimer of NOBA molecules in the above configuration increases the flexible tail of alkyl chains and that may help in forming a layered SmA structure[2]. Long alkyl chains also help in increasing the stability of SmA phase by decreasing the repulsive dipole-dipole interaction around the rigid cores by increasing the intermolecular distances[5]. Hence up to 50 mole percent of NOBA in the mixture all the above factors may be responsible for the appearance of SmA phase in the heating cycles. When concentration of NOBA molecules becomes approximately double of ChP, alternate strata of one ChP and two NOBA molecules rule out the possibility of the layered structure[19]. Perhaps the competition between ChP and NOBA molecules to form two different types of layered structure destroys the smectic layers.

From the transition temperatures and transition entropies of SmA and Ch phases in saturated cholesteryl esters, McMillan[20] found that as the alkyl chain increases the ratio $T_{red}(=T_{SmA-Ch}/T_{Ch-I})$ and the transition entropy $(\Delta S_{SmA-Ch})$ also increase. Variation of $T_{red}$ with mole percent of NOBA ($x$) for this mixture is shown in Figure 8 while that of transition entropy $\Delta S_{SmA-Ch}$ with $x$ is shown in Figure 5. From both these Figures, there seems to be a peak around $x=25$, thereby suggesting increase in chain length upto $x=25$ which happens to be in the eutectic region. For $x>25$, chain length decreases and at $x=56$, SmA phase becomes too weak to be observed by DSC. Lee *et al.*[21] extended the Kobayashi[22]–McMillan[20] model to SmA phase by separating the potential into spatial and orientational factors and could explain the variation of the transition entropy $\Delta S_{SmA-Ch}$ with the increasing reduced temperature $T_{red}$. For ChP + NOBA mixture, variations of $(\Delta S)_{SmA-Ch}$ with

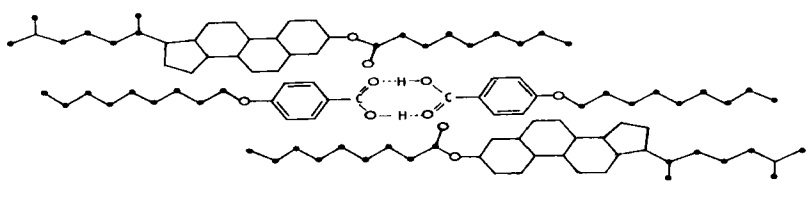

FIGURE 7 Packing arrangement of NOBA and ChP molecules in SmA phase of the mixture.

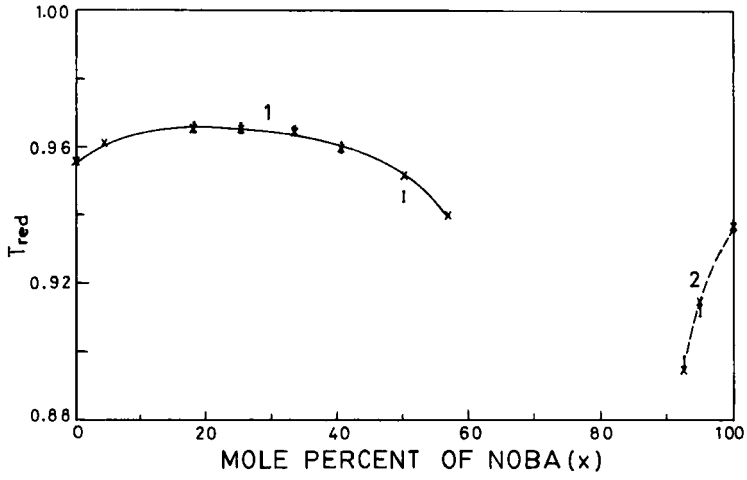


FIGURE 8 Variation of reduced temperature $T_{red}(= T_{Sm-Ch}/T_{Ch-I})$ with mole percent of NOBA ($x$). Curve 1 represents SmA phase and 2 SmC phase. Experimental data in heating are shown by (I) and in cooling by ($x$).

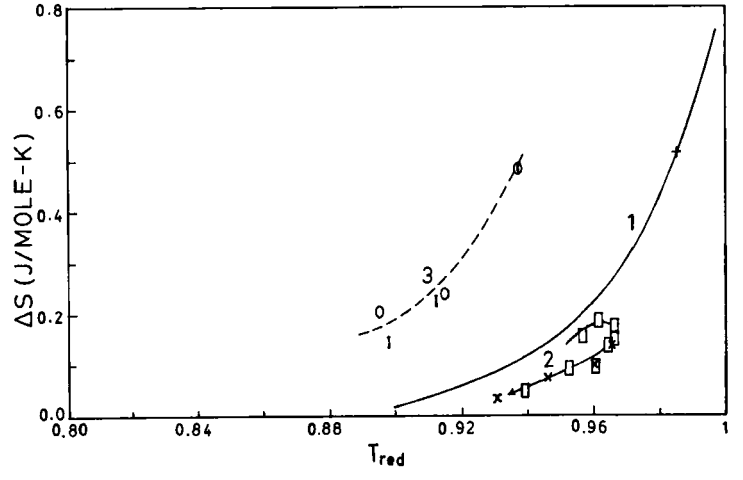


FIGURE 9 Variation of transition entropy with reduced temperature $T_{red}(= T_{Sm-Ch}/T_{Ch-I})$. Curve 1 represents the theoretical curve as calculated by Lee *et al.* Experimental data are shown on curve 2 for SmA-Ch phase (arrow shows increasing concentration of NOBA ($x$) and (+) for pure ChM)) and on curve 3 for SmC-Ch phase. For mixture, ($x$) represents SmA in heating, (□) SmA in cooling, ($I$) SmC in heating, ($O$) SmC cooling.

$T_{red}$ are shown as curve 2 in Figure 9. Although these data points lie below the theoretical curve of Lee *et al.*[21], increase in $\Delta S$ with $T_{red}$ is maintained in this mixture also. There is a turnover in $(\Delta S)_{SmA-Ch}$ with $T_{red}$ at 25 mole percent of

NOBA (see curve 2 Fig. 9) which lies in the eutectic region implying maximum chain length at this concentration.

## SmC Phase

In both heating and cooling, the transition temperatures of SmC phase decrease very rapidly with mole percent of ChP and SmC phase disappears at about 12 mole percent of ChP (see Fig. 1 (a) and (b)). Both the transition enthalpy and transition entropy of SmC phase decrease with concentration of ChP (see Fig. 4 and 5). For SmC phase also $\Delta S$ increases with $T_{red}$ (see curve 3 in Fig. 9). The theoretical curve as calculated by Lee *et al.*[21] is also shown as curve 1 in Figure 9 which lies below SmC phase and above SmA phase.

In SmC phase, the long axis of the molecules lie tilted at an angle to the layer interface. The molecular dipoles acting parallel to the major molecular axis enhance the thermal stability of this phase. Though the separation between the positive and negative charges of the molecular dipoles remains the same, due to the tilt of the molecules the positive and negative charges of the neighbouring molecules are brought nearer and at a suitable angle, the attractive forces may outweigh the repulsive forces and that causes the net energy of attraction to enhance the lateral attraction and hence the smectic properties[5].

The SmC phase is observed in pure NOBA and is destroyed by introducing low concentration of ChP. It seems that ChP molecules having length almost twice of NOBA molecules restrict the formation of layered SmC phase[19]. ChP molecules may decrease the thermal stability of SmC phase by increasing the average molecular lengths in SmC layers[23]. The suppression of SmC phase is also due to decrease in the orientational order because of disorientation of tilt directions caused by the interaction of longitudinal and lateral dipoles. NOBA molecules introduced into the ChP matrix assume the effective shape conforming to SmA phase, but not so by ChP molecules in NOBA matrix for SmC phase[1].

## CHOLESTERIC GAP

The range of the cholesteric phase is nearly constant from 0 to 50 mole percent of NOBA. It is widest (around 42 °C in heating and 50 °C in cooling) between 60 and 90 mole percent of NOBA in both heating and cooling. The range of the cholesteric phase is large in the absence of the smectic phases. That may be due to the rapid decrease of the translational order parameter in the smectic layers causing the formation of the cholesteric phase where the molecules can migrate freely[19]. The transition temperature (73.5 °C) and enthalpy (0.85 J/gm) of pure ChP are lower than the transition temperature (77.1 °C) and enthalpy (2.44 J/gm) of pure cholesteryl myristate (ChM)[24] for Ch-SmA phase transition, and the cholesteric gap of ChP-NOBA system is wider than those of ChM-NOBA system[1]. This kind of relationship has also been observed by Dabrowski[2] according to whom lower the SmA-N

phase transition temperature and smaller the enthalpy of this transition, wider is the nematic gap. Range of the cholesteric phase in pure ChP (15.8 °C) is also larger than the range of the cholesteric phase in pure ChM (5.5 °C).

The cholesteric to isotropic (Ch-I) transition temperature increases with the increasing concentration of NOBA and almost reaches linearly to the nematic to isotropic (N-I) transition temperature of pure NOBA (see Fig. 1 (a) and (b)). It may also be noted that maximum depression in Ch-I and I-Ch transition temperatures occur at 33.3 mole percent of NOBA, which lies in the eutectic region of the mixture (see Fig. 1 (a) and (b)).

The enthalpy ($\Delta H$) and entropy ($\Delta S$) of Ch-I transitions could be fitted on the following equations

$$\Delta H = x_1 \Delta H_1 + x_2 \Delta H_2 + A_H (x_1 \Delta H_1 x_2 \Delta H_2)^{(1/2)} \tag{3}$$

$$\Delta S = x_1 \Delta S_1 + x_2 \Delta S_2 + A_S (x_1 \Delta S_1 x_2 \Delta S_2)^{(1/2)} \tag{4}$$

where $x_1, \Delta H_1$ and $\Delta S_1$ are the mole fraction, enthalpy and entropy of pure ChP and $x_2, \Delta H_2$ and $\Delta S_2$ are the respective parameters of pure NOBA. Constants $A_H$ and $A_S$ in the above equations are the mixing parameters and the best fit values are $A_H = -0.37 \pm 0.14$ and $A_S = -0.26 \pm 0.13$ showing deviation from ideal mixing. In Figure 10 and 11 the plots of equation (3) and (4) are given alongwith the experimental points. Finite negative values of $A_H$ and $A_S$ show that two components of the mixture interact to produce excess disordering in the system and destabilize Ch phase. Negative mixing term of enthalpy is observed by several other workers also e.g. Dabrowski *et al.* in the binary system of 4DBT-10TPCHB [19]. SmA-I transition

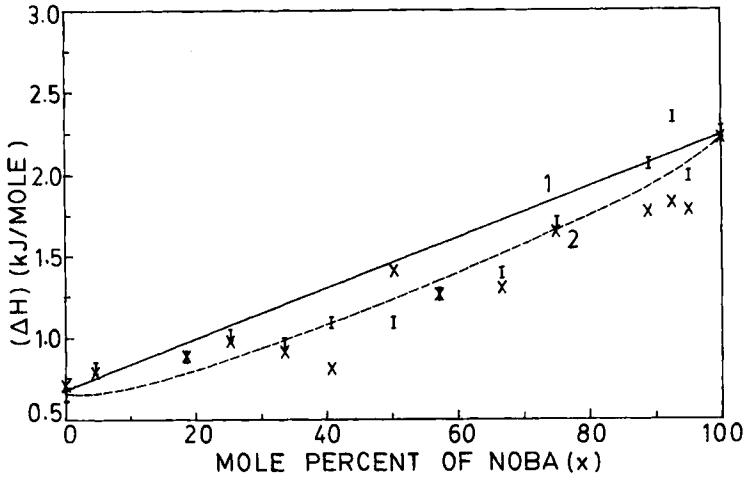


FIGURE 10 Transition enthalpy as a function of mole percent of NOBA ($x$) for Ch-I (I-Ch) transition. Curve 1 represents the theoretical plot of equation (1) with mixing parameter $A_H = 0$, curve 2 with $A_H = -0.37$. Experimental data in heating are shown by (I) and in cooling by (x).

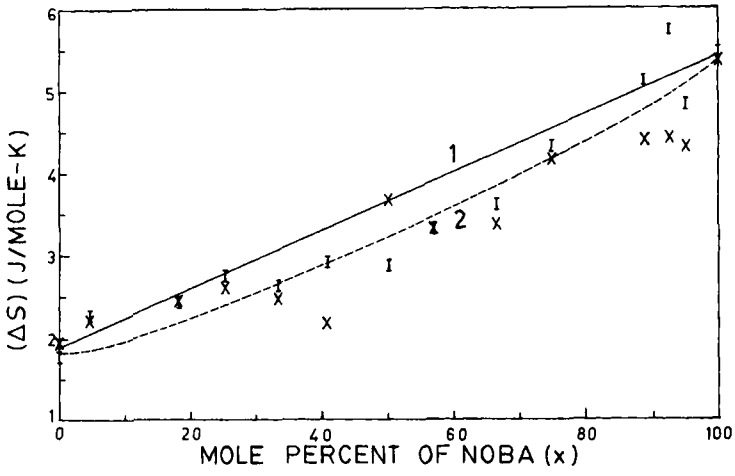


FIGURE 11 Transition entropy as a function of mole percent of NOBA ($x$) for Ch-I (I-Ch) transition. Curve 1 represents the theoretical plot of equation (2) with mixing parameter $A_S = 0$, curve 2 with $A_S = -0.26$. Experimental data in heating are shown by (I) and in cooling by ($x$).

enthalpy also shows negative mixing term and according to Dabrowski *et al.*[19] this is the manifestation of decrease in the smectic lattice energy.

## WIDTH OF TRANSITIONS

Onset temperature $T_{ON}$ of a thermogram represents the intersection point of the slope of the leading edge with the baseline which corresponds to 20% to 30% of the total peak height for almost all the transition processes.

The half-width of a transition process $\Delta T$ may be taken as $(T_P - T_{ON})$ where $T_P$ is the peak transition temperature. Half-widths of (Ch-I), (K–K′) and (K′-Mesophase) transitions at the scanning rate of 5 °C/min as a function of mole percent of NOBA ($x$) are shown in Figure 12 which shows a maximum at $x = 66 \pm 0.4\%$. It may be noted that for all phase transitions in the mixture, $\Delta T$ is larger than of pure components. It is also observed that the half-width of (Ch-I) transition increases linearly with scanning rate (see Fig. 13).

## VAN'T HOFF EQUATION

The Van't Hoff equation[25]

$$x = (\Delta H \delta T_p)/(R T_p^2) \tag{5}$$

has been applied to calculate the impurity concentrations ($x$) from the melting and freezing thermograms (see Tab. 2), where $R$ is the gas constant in $J$/(mole-K), $T_p$ the melting point in $K$, $\Delta H$ the transition enthalpy in $J$/mole of the pure material and

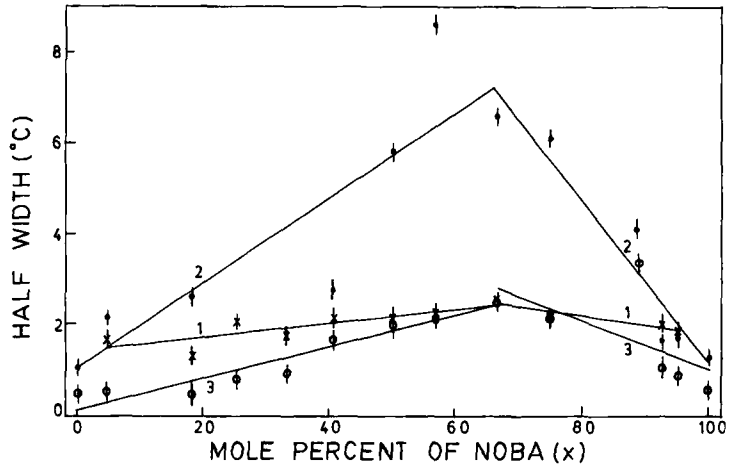


FIGURE 12 Half-width $\Delta T (= T_p - T_{ON})$ of various transitions as a function of mole percent of NOBA in heating. Curve 1 represents K-K′ transition, curve 2 K′-Mesophase transition and curve 3 Ch-I transition. Experimental data for K-K′ transition are shown by (x), for K′-Mesophase transition by (●) and for Ch-I transition by (*O*).

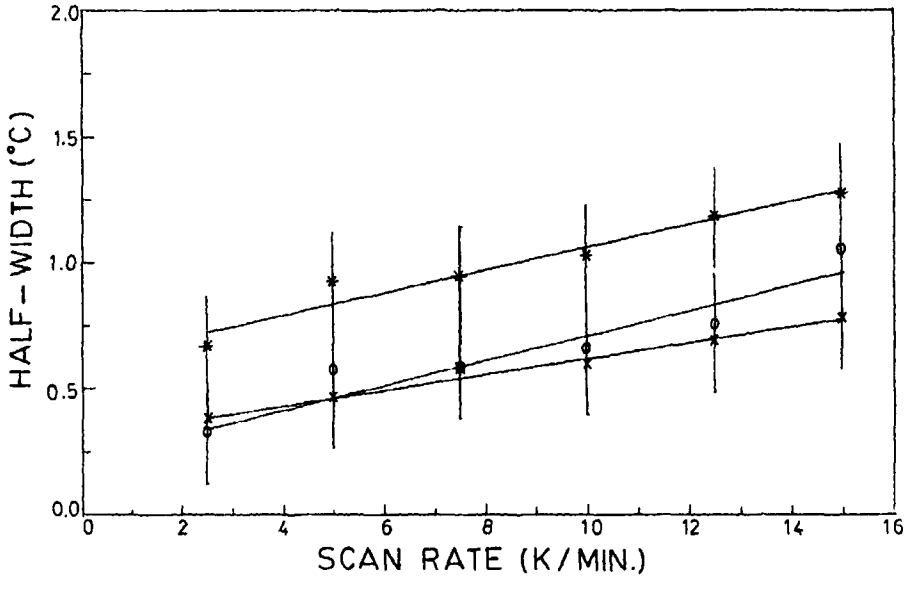


FIGURE 13 Half-width $\Delta T (= T_p - T_{ON})$ of Ch-I transition with scanning rate. Experimental data for 33 mole percent of NOBA are shown by (*), for pure NOBA by (*O*), for pure ChP by (x).

$\delta T_p$ is the crystal to mesophase transition temperature depression due to impurity. From Table 2 it is observed that the calculated impurities agree with the experimental values for impurities of ChP in NOBA upto 7.5 mole percent (within $\pm$ 10%) when we use the freezing crystallization data in equation (5). From the melting data

TABLE 2
Mole percent of impurities from Van't Hoff equation.

| *Pure component* | *Added Impurity* | | *Calculated Impurity* | |
|---|---|---|---|---|
| | | | *K'-Meso·* | *Meso-K'* |
| NOBA | ChP | 4.9 | 2.7 | 5.4 |
| NOBA | ChP | 7.45 | 3.5 | 6.7 |
| NOBA | ChP | 11.14 | 8.1 | 8.9 |
| ChP | NOBA | 4.67 | 2.0 | — |

of crystal-meso phase transition, even for such low concentration of impurities the calculated values are lower than the experimental values by 50%. The impurity of NOBA in ChP could not be calculated from cooling run of DSC data, because we did not observe crystallization upto room temperature.

In the binary mixtures of ChP and NOBA eutectic composition divides the system in two regions. One below the eutectic composition, where the properties of ChP dominates and the stability of SmA phase is enhanced due to addition of NOBA in the matrix of ChP molecules and SmA* phase is also induced. Other region is above the eutectic composition where properties of NOBA dominates but stability of SmC phase decreases due to addition of ChP in the matrix of NOBA molecules. Both the regions are separated by a large cholesteric gap observed between 60 and 90 mole percent of NOBA where miscibility of NOBA and ChP molecules is completely broken.

We may therefore summarize the results as below

(1) Addition of small concentration of NOBA stabilizes SmA phase of ChP making it enantiotropic.
(2) On addition of about 10 mole percent of ChP in NOBA, SmC phase gets suppressed.
(3) The eutectic point of this mixture is observed at $28 \pm 2$ mole percent of NOBA.
(4) A very large cholesteric range 42 °C is obtained in heating and 50 °C in cooling at 90 mole percent of NOBA.
(5) For both enthalpy and entropy of Ch-I transitions mixing terms are negative.
(6) For all the transitions, widths of the transitions for the mixture are larger than that of the pure components. More so, mixed cyrstal phase to mesophase transition seems to be broadest of all.
(7) Concentrations of impurities of less than 10 mole percent can be determined by the Van't Hoff equation from the thermodynamic data of freezing crystallization.

**Acknowledgements**

We thank Dr. O. D. Lavrentovich of Institute of Physics, Kiev, Ukraina for providing us pure grade liquid crystal materials and the University Grants Commision, New Delhi for financial assistance under COSIST programme and a research project grant. One of us (RD) thanks to University Grants Commission, New Delhi for the award of a senior research fellowship.

## References


1. L. N. Lisetsky, L. A. Batrachenko, V. D. Panikarskaya, *Mol. Cryst. Liq. Cryst.*, **215**, 287 (1992).
2. R. Dabrowski, K. Czuprynski, J. Przedmojski, B. Wazynska, *Liq. Cryst.*, **14**, 1359 (1993).
3. O. D. Lavrentovich, Y. A. Nastishin, *Ukr. Fiz. Zhurnal*, **35**, 221 (1990) (In Russian).
4. O D. Lavrentovich, Y. A. Nastishin, V. I. Kulishov, Y. S. Narkevich, A. S. Tolochko, S. V. Shiyanovskii, *Europhysics Letters*, **13 (4)**, 313 (1990).
5. S. Takenaka, M. Koden, S. Kusabayashi, *J. Phys. Chem.*, **90**, 666 (1986).
6. K. A. Suresh, *Mol. Cryst. Liq. Cryst.*, **97**, 417 (1983).
7. D. F. Aliev, G. M. Bairamov, R. M. Cherkashina, *Sov. Phys. Crystallogr.*, **32**, 715 (1987).
8. A. J. Palangana, S. Jayaraman, T. Kroin, *Mol. Cryst. Liq. Cryst.*, **131**, 217 (1985).
9. S. L. Srivastava, V. K. Agrawal, *Nat. Acad. Sci. Lett.*, **13**, 243 (1990).
10. K. S. Kunihisa, Y. Satomi, *Mol. Cryst. Liq. Cryst.*, **141**, 1 (1986).
11. E. C. H. Hsu, J. F. Johnson, *Mol. Cryst. Liq. Cryst.*, **27**, 95 (1974).
12. D. Demus, Ch. Fietkau, R. Schubert, H. Kehlen, *Mol. Cryst. Liq. Cryst.*, **25**, 215 (1974).
13. V. A. Molochko, S. P. Naumenkov, S. M. Pestov, *Mol. Mat.*, **2**, 57 (1992).
14. J. W. Goodby, *Mol. Cryst. Liq. Cryst.*, **75**, 179 (1981).
15. J. S. Dave, R. A. Vora, Liquid Crystals and Plastic Crystals, vol. 1, ed by G. W. Gray, P. A. Winsor, John Wiley & Sons, New York **153**, (1979).
16. N. C. Shivaprakash, Molecular Structure and Physical Properties of Liquid Crystals, Ph.D. thesis submitted to Physics Department, Mysore University, Mysore, 1981.
17. L. S. Chou, E. F. Carr, *Phys. Rev.*, **A 7**, 1639 (1973).
18. P. Patel, S. Kumar, P. Ukleja, *Liq Cryst.*, **16**, 351 (1994).
19. R. Dabrowski, B. Wazynska, B. Sosnowska, *Liq. Cryst.*, **1**, 415 (1986).
20. W. L. McMillan, *Phys. Rev.*, **A 4**, 1238 (1971).
21. F. T. Lee, H. T. Tan, Y. M. Shih, C. W. Woo, *Phys. Rev. Lett.*, **31**, 1117 (1973).
22. K. K. Kobayashi, *J. Phys. Soc. Japan*, **29**, 101 (1970).
23. D. Coates, *Liq. Cryst.*, **2**, 63 (1987).
24. S. L. Srivastava, R. Dhar, M. V. Kurik, *Mol. Mat.*, **2**, 261 (1993).
25. E. M. Barrall, M. J. Vogel, *Thermochim. Acta*, **1**, 127 (1970).